



# Molecular Docking Studies on Various Food Grades Dyes as a Potential Inhibitor of COVID-19

Pankaj Dagur and Manik Ghosh \*

Department of Pharmaceutical Sciences and Technology, Birla Institute of Technology, Mesra 835215, Jharkhand, India

\* Correspondence: manik@bitmesra.ac.in

† Presented at the 24th International Electronic Conference on Synthetic Organic Chemistry, 15 November–15 December 2020; Available online: <https://ecsoc-24.sciforum.net/>.

Received: date; Accepted: date; Published: date

**Abstract:** In December 2019, the Coronavirus disease-2019 (COVID-19) virus had emerged in Wuhan, China. The first resolved COVID-19 crystal structure (main protease) has been developed and various repurposing activities are in process. In this study, a knowledge gap in relations of COVID-19 with the previously known fatal Coronaviruses (CoVs) epidemics, SARS and MERS CoVs, has been covered by investigation of sequence statistics, molecular modelling, virtual screening, docking and sequence comparison statistics of the COVID-19 main protease. COVID-19 Mpro formed a sequence similarity group with SARS CoV that was distant from MERS CoV. The identity % was 96 and 51 for COVID-19/SARS and COVID-19/MERS CoV sequence comparisons, respectively. We have used molecular docking and molecular interaction approach to identify small-molecules which bind to the isolated Viral S-protein at its host receptor region. These molecules have good solubility and pharmacodynamics properties They also obeyed Lipinski's rule, which makes them promising compounds to pursue further biochemical and cell-based assays to explore their potential for use against nCOVID-19. We hypothesize that the top score identified molecules may be used to limit viral recognition of host cells and/or disrupt host-virus interactions. A ranked list of selected compounds is given that can be tested experimentally.

**Keywords:** COVID-19; SARS CoV; MERS CoV; Docking

---

## 1. Introduction

On the penultimate day of 2019, health officials at the Wuhan Municipal Health Commission (Hubei Province, China) reported an occurrence of concentrated pneumonia in the city of Wuhan. Shortly after reporting the outbreak the Chinese Centre for Disease Control (Chinese CDC) and local Chinese health workers determined that the cause of the outbreak was a novel coronavirus i.e., nCov-2019 [1–3]. Then on 11th of March 2020, WHO declared it as pandemic. The symptoms of Coronavirus (COVID-19) Infection are mild respiratory symptoms and fever that occurs on an average of 5–6 days after infection (mean incubation period 5–6 days, range 1–14 days) [4,5]. The current treatment options are use of antivirals and antimalarials. The first available crystal structure of COVID-19 proteins is Mpro, which was published in February 2020 (PDB ID 6lu7). In this study, the first virtual screening study against the first known COVID-19 was performed. The obtained results will help in identifying some potential inhibitors to combat the recent dangerous COVID-19. We propose to use food grade dyes that could acts as a treatment option in case of COVID-19 patients. We have used computational methods i.e., molecular docking to evaluate the activity as well as the interactions.

## 2. Materials and Methods

### 2.1. Retrieval of Mpro Sequences

The NCBI GenBank or GISAID (<https://www.gisaid.org/>) were used to obtain the COVID-19 sequences. SARS CoV and MERS CoV sequences were obtained from the GenBank [7,8].

### 2.2. Sequence Alignment and Multiple Sequence Comparisons

Pairwise and multiple sequence comparisons of Mpro were done using CLC genomics software (Qiagen Inc., USA). The sequence comparison matrix was generated, including the number of gaps, number of different residues and identity %.

Sequences alignment of Mpro from SARS CoV, MERS CoV and COVID-19.

(A) Pairwise with dots for identities sequence alignment of COVID-19 and SARS CoVs

#### Identities 294/306 (96%)

SARS Mpro 2AMD	SGFRKMAFSPGKVEGCMVQVTCGTTTLNGLWLDLDTVYCPRHVICTAEDMLNPNYEDLLIR	65
COVID-19 Mpro YP_009725301	.....V.....S.....	60
SARS Mpro 2AMD	KSNHSFLVQAGNVQLRVIGHSMQNCLLRKVDTSNPKTPKYKFVRIQPGQTFVSLACYNG	125
COVID-19 Mpro YP_009725301	...N.....V.K.....A.....	120
SARS Mpro 2AMD	SPSGVYQCAMPNHTIKGSFLNGSCGSGVGFNIDYDCVSFCYMHMELPTGVHAGTDLEGK	185
COVID-19 Mpro YP_009725301	.....F.....N	180
SARS Mpro 2AMD	FYGPFDVDRQTAQAAGTDTTITLNLVLAWLYAAVINGDRWFLNRFTTTLNDFNLVAMKYNYE	245
COVID-19 Mpro YP_009725301	.....V.....	240
SARS Mpro 2AMD	PLTQDHVDILGPLSAQTGIAVLDMCAALKELLQNGMNGRTILGSTILEDEFTPFVVRQC	305
COVID-19 Mpro YP_009725301	.....S.....AL.....	300
SARS Mpro 2AMD	SGVTFQ	311
COVID-19 Mpro YP_009725301	.....	306

(B) Pairwise with dots for identities sequence comparison of COVID-19 and MERS CoVs.

#### Identities 157/310 (51%)

MERS Mpro 5C3N	SGLVKMSPSGDVEACMVQVTCGSMTLNGLWLDNTVWCPRHVMCPADQLSDPNYDALLIS	60
COVID-19 Mpro YP_009725301	..FR..AF...K..G.....TT.....DV.Y....I.TSEDMLN...ED...R	60
MERS Mpro 5C3N	MTNHSFSVQKHIGAPANLRVVGHAMQGTLLKLTVDVANPSTPAYTFTTVKPGAFAFVSLAC	120
COVID-19 Mpro YP_009725301	KS..N.L.--AGNVQ...I..S..NCV...K..T...K..K.K.VRIQ..QT.....	117
MERS Mpro 5C3N	YNGRPTGTFTVVMRPNYTIKGSFLCGSCGSGVGTKEGVSINFCYMHQOMELANGHTGSAF	180
COVID-19 Mpro YP_009725301	...S.S.VYQCA...F.....N.....FNIDYDCVS.....H...PT.V.A.TDL	177
MERS Mpro 5C3N	DGTMYGAFMDKQVHQVQLTDKYCSVNVVAWLYAAILNGCAWFKPNRTSVVVFNEWALAN	240

COVID-19 Mpro YP\_009725301 E.NF..P.V.R.TA.AAG..TTIT...L.....VI..DR..LNRFT.TLND..LV.MKY 237

MERS Mpro 5C3N QFTEFVGTQSVDM---LAVKTGVAIEQLLYAIQQLY-TGFQKQILGSTMLEDEFTPEDV 296

COVID-19 Mpro YP\_009725301 NY-.PLTQDH..ILGP.SAQ..I.VLDMCASLKE.LQN.MN.RT....AL.....F.. 296

MERS Mpro 5C3N NMQIMGVVMQ 306

COVID-19 mpro YP\_009725301 VR.CS..TF. 306

### 2.3. Docking

The structure of COVID-19 virus Mpro in complex with N3 provides a model for identifying lead inhibitors to target COVID-19 virus Mpro through in silico screening. We have used molecular docking approach to predict the binding energy and inhibition constants of various food grade dyes under study [9,10]. We docked our ligands into the main protease of COVID-19 and screened them for their activity against COVID-19.

### 2.4. Predictive ADME Studies

Predictive ADME studies were performed by using Swiss tools\*. It is an online tool that requires the structure or the smiles for calculating the parameters.

The test compounds were built within the window by using the drawing tools of the online server else smiles can be directly copied instead of drawing structures[11].To assure drug like pharmacokinetic profile in rational drug designing, predictive ADME calculations are done on the basis of Lipinski's rule of five.

### 2.5. Toxicity

The toxicity of the molecules were predicted by using Toxtree [12], a free offline tool available for the prediction of toxicity. It requires the smiles format of structures to calculate the toxicity.

The smiles format of the compounds were pasted in the chemical identifier bar, and then their toxicity was estimated on the basis of creamer rules. The Compounds are categorised into three classes, i.e., Low (Class I), Intermediate (Class II) and High (Class III).

## 3. Results & Discussions

### 3.1. Docking

The PDB ID of protein used was 6LU7 which was retrieved from Protein data bank. The validation of the model was performed was redocking the internal ligand/inhibitor into the active site of the macromolecule. Then the individual ligands were prepared in Auto Dock 4.2.6 software as per standard protocols and docking was carried out. The results are listed below Table 1 and Figures 1–5

**Table 1.** List of Ligands with binding energy and inhibition constants.

S. No.	Ligands	1st Run		2nd Run		3rd Run	
		Binding Energy	Inhibition Constant	Binding Energy	Inhibition Constant	Binding Energy	Inhibition Constant
1	DG01	-10.35	26.12 nM	-9.99	47.43 nM	-9.91	54.73 nM
2	DG02	-9.52	104.45 nM	-9.07	225.6 nM	-8.99	259.33 nM
3	DG03	-9.43	121.71 nM	-9.29	154.77 nM	-9.28	158.05 nM

4	DG04	-9.1	214.18 nM	-8.98	261.41 nM	-8.66	447.14 nM
5	DG05	-9.00	251.81 nM	-8.89	305.47	-8.87	314.38 nM
6	DG06	-8.86	322.93 nM	-8.63	472.32 nM	-8.63	475.09 nM
7	DG07	-8.53	555.76 nM	-8.53	561.87 nM	-8.52	571.48 nM
8	DG08	-7.97	1.44 uM	-7.6	2.67 uM	-7.11	6.1 uM
9	DG09	-7.86	1.73 uM	-7.72	2.2 uM	-7.63	2.54 uM
10	DG10	-7.81	1.87 uM	-7.81	1.87 uM	-7.80	1.92 uM
11	DG11	-7.42	3.63 uM	-7.33	4.24 uM	-7.28	4.6 uM
12	DG12	-7.35	4.12 uM	-6.33	22.87 uM	-6.30	24.27 uM
13	DG13	-7.34	4.14 uM	-7.28	4.62 uM	-7.32	4.32 uM
14	DG14	-6.14	31.82 uM	-6.13	31.97 uM	-6.12	32.46 uM
15	DG15	-6.24	26.75 uM	-4.79	307.68 uM	-5.78	58.44 uM

### 3.2. Predictive ADME Studies

Analysis of all the compounds was done for the physicochemically and pharmacokinetically important descriptors using SWISS tools. In order to predict the drug-alike properties of molecules these major descriptors are required.

These properties are

- Molecular weight (mol MW) (150–650)
- Octanol/water partition coefficient (Log Po/w) (-2–6.5)
- Hydrogen Bond Donor ( $\leq 5$ )
- Hydrogen Bond Acceptor ( $\leq 10$ )
- Human oral absorption percentage ( $\geq 80\%$  is high,  $\leq 25\%$  is poor)

The entire set of compounds showed appreciable values for the properties analyzed as well as exhibited drug alike aspects based on Lipinski's rule of five. The results are summarised in Table 2.

**Table 2.** Swiss ADME for compounds DG01-15.

<b>Compounds Properties</b>	<b>DG01</b>	<b>DG02</b>	<b>DG03</b>	<b>DG04</b>	<b>DG05</b>	<b>DG06</b>	<b>DG07</b>	<b>DG08</b>	<b>DG09</b>	<b>DG10</b>	<b>DG11</b>	<b>DG12</b>	<b>DG13</b>	<b>DG14</b>	<b>DG15</b>
<b>M.W</b>	546.53	538.53	835.89	537.43	496.38	458.46	273.29	561.69	539.4	314.25	468.42	408.41	422.39	495.39	538.41
<b>HBA</b>	11	11	5	12	12	9	3	7	14	7	12	9	8	12	13
<b>HBD</b>	3	4	2	8	8	3	0	3	9	4	3	3	4	8	7
<b>M.R</b>	138.93	123.99	139.61	131.61	120.15	113.81	79.7	149.36	128.28	77.74	109.69	96.31	101.04	121.7	129.89
<b>TPSA</b>	208.86	229.71	75.99	238.99	230.12	170.45	47.03	-1.14	273.21	132.13	220.19	170.45	183.7	235.91	236.19
<b>LOG Po/w</b>	1.54	1.37	5.23	-1.25	-1.25	2.8	2.05	2.94	-4	0	0.32	2.02	-0.18	-0.71	-0.31
<b>Solubility (mg/ml)</b>	1.13 × 10 <sup>-2</sup>	6.97 × 10 <sup>-2</sup>	4.44 × 10 <sup>-7</sup>	6.15 × 10 <sup>-3</sup>	7.05 × 10 <sup>-3</sup>	4.58 × 10 <sup>-3</sup>	6.63 × 10 <sup>-3</sup>	4.22 × 10 <sup>-6</sup>	3.51 × 10 <sup>-1</sup>	4.22 × 10 <sup>-2</sup>	5.74 × 10 <sup>-1</sup>	5.59 × 10 <sup>-2</sup>	1.63 × 10 <sup>-1</sup>	5.74 × 10 <sup>-4</sup>	2.90 × 10 <sup>-3</sup>
<b>G.I absorption</b>	Low	Low	High	Low	Low	Low	High	Low	Low	High	Low	Low	Low	Low	Low
<b>BBB Permeant</b>	No	No	No	No	No	No	Yes	No							
<b>CYP1A2</b>	No	No	Yes	No	Yes	No	Yes	No	No	No	No	No	No	Yes	Yes
<b>CYP2D6</b>	No														
<b>Veber</b>	No	Yes	Yes	No	No	No	Yes	No	No	Yes	No	No	No	No	No
<b>Lipinski</b>	No	No	No	No	No	Yes	Yes	No	No	Yes	No	Yes	Yes	No	No
<b>Bioavailability Score</b>	0.11	0.11	0.17	0.11	0.11	0.11	0.55	0.11	0.11	0.56	0.11	0.11	0.11	0.11	0.11

M.W: Molecular weight, HBA: Hydrogen bond acceptor, HBD: Hydrogen bond donor, TPSA: Total polar surface area, Log Po/w: Octanol/water partition coefficient, Log S: Aqueous solubility, MR: Molar Refractivity, CYP1A2: Cytochrome P450 1A2, CYP2D6: Cytochrome P450 2D6.



### 3.3. Toxicity

Toxicity prediction of the compounds is necessary, before further development. The toxicity is predicted by using Craemer rules. It categorises the compounds into the classes, i.e., Low (Class I), Intermediate (Class II) and High (Class III), depending upon its toxicity index. The categories are based upon different threshold of toxicological concern, these are as follows-

- Class I- 1,800 (30  $\mu\text{g}/\text{kg}$  bw/d)
- Class II- 540 (9  $\mu\text{g}/\text{kg}$  bw/d)
- Class III- 90 (1.5  $\mu\text{g}/\text{kg}$  bw/d)

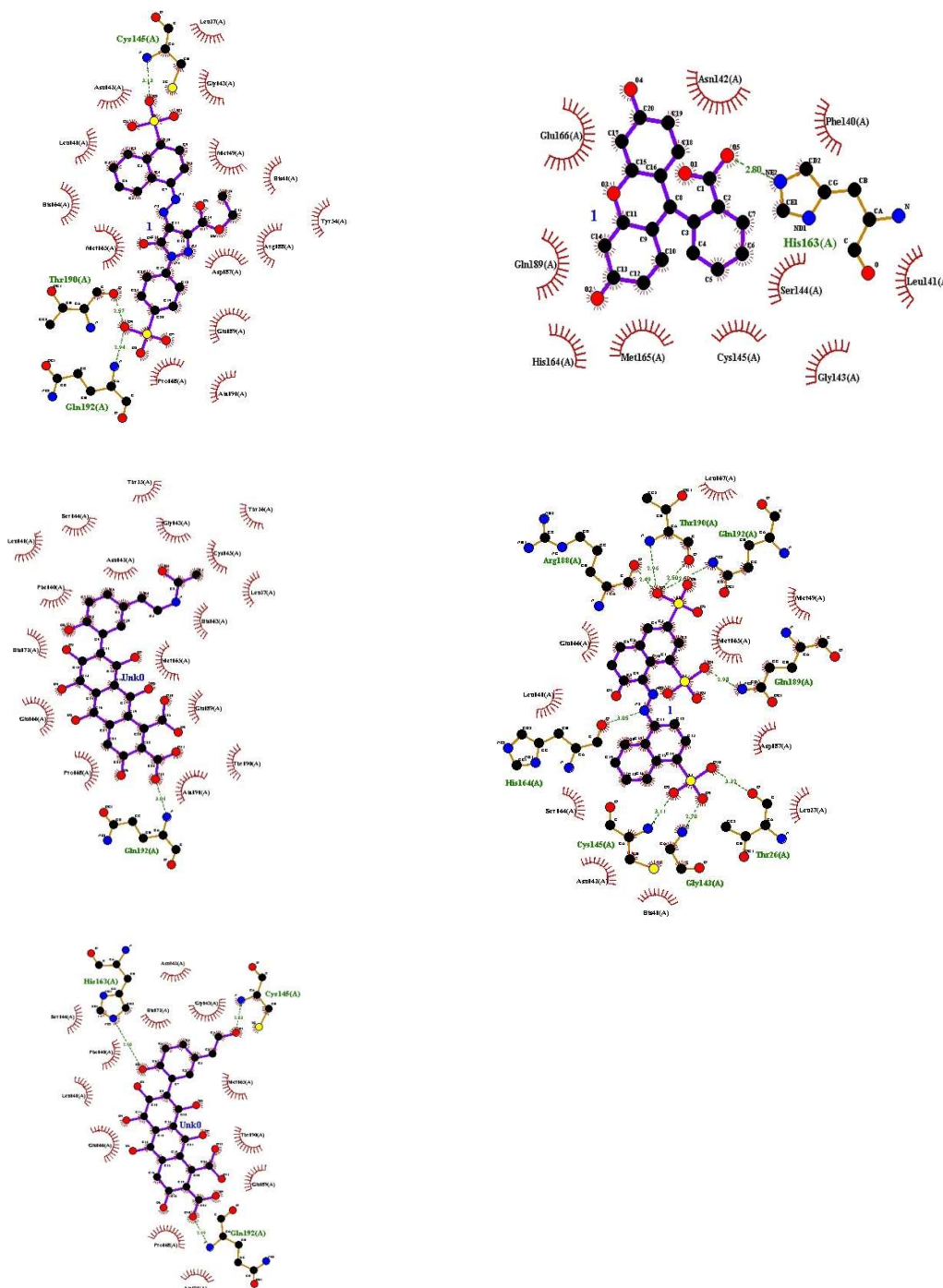
The results are summarised in Table 3.

**Table 3.** Toxicity of the compounds DG01-15.

Compounds	Toxicity Class
DG01	High Class III
DG02	Low Class I
DG03	High Class III
DG04	High Class III
DG05	High Class III
DG06	Low Class I
DG07	High Class III
DG08	Low Class I
DG09	High Class III
DG10	High Class III
DG11	Low Class I
DG12	Low Class I
DG13	Low Class I
DG14	High Class III
DG15	High Class III

From the ADME studies it was found that only few compounds followed all the parameters for being a suitable drug candidate, but all the other compounds violated the parameters by a few factors, which on further modifications can be modified to promising drug candidates. The toxicity studies suggests that, the therapeutic range of some compounds is very narrow, whereas some have wide therapeutic ranges, these can be modified as per the purpose. The modifications required can be taken as a future perspective to develop these compounds as promising drug candidates.

### Docking Interactions



1. Orange B 2. Cochineal Red A 3. Erythrosine 4. Laccaic acid A 5. Laccaic acid B

#### 4. Conclusions

Researchers are now focusing mainly on synthetic protease inhibitors, but natural compounds have always been found better than synthetic counterparts. We being natural chemists have tried to focus on untouched natural drugs that could provide better drug therapies in the future. As per our study, the sequence identity % was 96 and 51 for COVID-19/SARS and COVID-19/MERS CoV, respectively. Docking studies revealed that Orange B (-10.35 kcal/mol) and Cochineal Red A (-9.52 kcal/mol) had the best binding affinity with the receptor. They had low GI absorption but they showed no BBB permeation activity. They obeyed Lipinski rule and bioavailability score was 0.11, and showed drug alike aspects. Cochineal Red A was classified under Low Class I toxicity.

Erythrosine, Laccaic Acid A, Laccaic Acid B, Azorubine and Quinoline yellow also had a comparable binding affinity. These two molecules/compounds proved to be a good inhibitor against the COVID-19 main protease. Further MD simulation studies can be performed to mimic their interaction with the receptor. These molecules can further be studied for their in-vitro and in-vivo activity. This work may pave a new path for the development of potential drugs using food grade dyes and for the selection of compounds as well as designing new scaffolds or novel combinatorial libraries of analogs/derivatives but before coming to any outcome of an in-silico study, proper in-vitro and in-vivo research works should be performed.

**Acknowledgments:** The authors would like to thank the Head, Department of Pharmaceutical Sciences and Technology, BIT, Mesra for providing the research facilities for performing the current study.

**Conflicts of Interest:** There is no conflict of interest.

## References

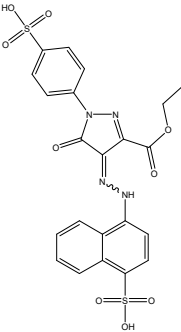
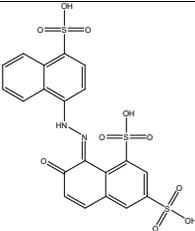
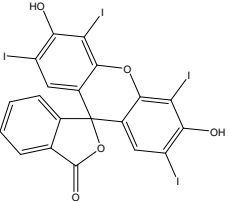
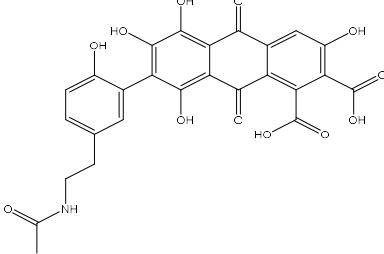
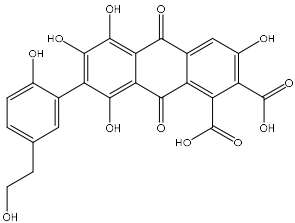
1. Xu, X.; Chen, P.; Wang, J.; Feng, J.; Zhou, H.; Li, X.; Zhong, W.; Hao, P. Evolution of the novel coronavirus from the ongoing Wuhan outbreak and modeling of its spike protein for risk of human transmission. *Sci. China Life Sci.* **2020**, *63*, 457–460, doi:10.1007/s11427-020-1637-5.
2. Peiris, J.S.M.; Lai, S.T.; Poon, L.L.M.; Guan, Y.; Yam, L.Y.C.; Lim, W.; Nicholls, J.; Yee, W.K.S.; Yan, W.W.; Cheung, M.T.; et al. Coronavirus as a possible cause of severe acute respiratory syndrome. *Lancet* **2003**, *361*, 1319–1325, doi:10.1016/s0140-6736(03)13077-2.
3. Li, W.; Wong, S.-K.; Li, F.; Kuhn, J.H.; Huang, I.-C.; Choe, H.; Farzan, M. Animal Origins of the Severe Acute Respiratory Syndrome Coronavirus: Insight from ACE2-S-Protein Interactions. *J. Virol.* **2006**, *80*, 4211–4219, doi:10.1128/jvi.80.9.4211-4219.2006.
4. Zaki, A.; Van Boheemen, S.; Bestebroer, T.; Osterhaus, A.; Fouchier, R. Isolation of a Novel Coronavirus from a Man with Pneumonia in Saudi Arabia. *New Engl. J. Med.* **2012**, *367*, 1814–1820, doi:10.1056/nejmoa1211721.
5. Desenclos, J.C.; Van der Werf, S.; Bonmarin, I.; Levy-Bruhl, D.; Yazdanpanah, Y.; Hoen, B. Introduction of SARS in France, March–April, 2003. *Emerg. Infect. Dis.* **2004**, *10*, 195.
6. Guarner, J. Three Emerging Coronaviruses in Two Decades. *Am. J. Clin. Pathol.* **2020**, *153*, 420–421, doi:10.1093/ajcp/aqaa029.
7. Wan, Y.; Shang, J.; Graham, R.; Baric, R.S.; Li, F. Receptor Recognition by the Novel Coronavirus from Wuhan: an Analysis Based on Decade-Long Structural Studies of SARS Coronavirus. *J. Virol.* **2020**, *94*, 27–20, doi:10.1128/jvi.00127-20.
8. Hilgenfeld, R. From SARS to MERS: crystallographic studies on coronavirus pro-teases enable antiviral drug design. *FEBS J.* **2014**, *281*, 4085–4096.
9. Kandeel, M.; Altaher, A.A.; Alnazawi, M. Molecular Dynamics and Inhibition of MERS CoV Papain-like Protease by Small Molecule Imidazole and Aminopurine Derivatives. *Lett. Drug Des. Discov.* **2019**, *16*, 584–591, doi:10.2174/1570180815666180918161922.
10. Li, Y.-H.; Hu, C.-Y.; Wu, N.-P.; Yao, H.; Li, L. Molecular Characteristics, Functions, and Related Pathogenicity of MERS-CoV Proteins. *Engineering* **2019**, *5*, 940–947, doi:10.1016/j.eng.2018.11.035.
11. Available online: <http://www.swissadme.ch> (accessed on 15 October 2020).
12. Patlewicz, G.; Jeliaskova, N.; Safford, R.J.; Worth, A.P.; Aleksiev, B. An evaluation of the implementation of the Cramer classification scheme in the Toxtree software. *SAR QSAR Environ. Res.* **2008**, *19*, 495–524, doi:10.1080/10629360802083871.

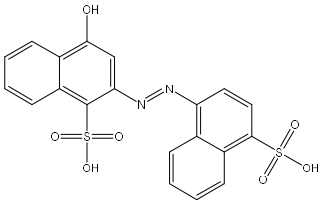
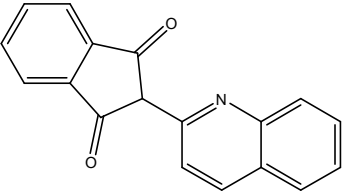
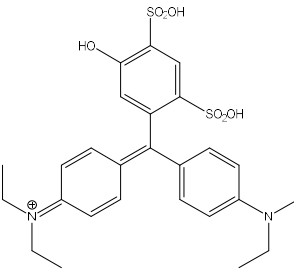
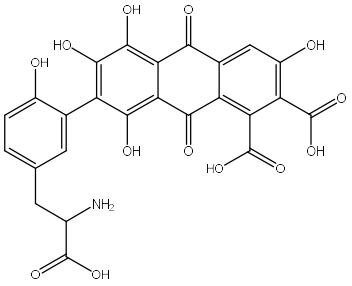
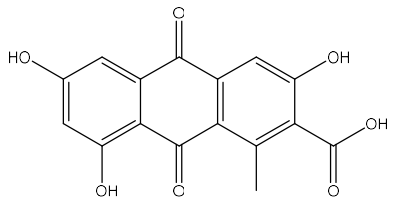
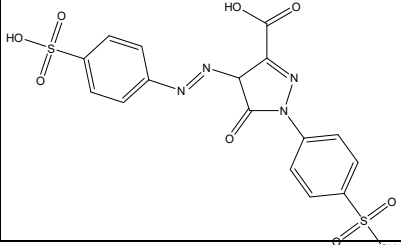
**Publisher's Note:** MDPI stays neutral with regard to jurisdictional claims in published maps and institutional affiliations.

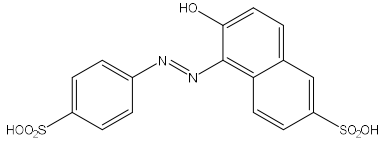
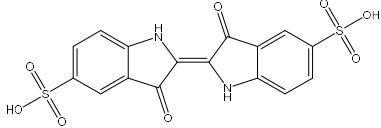
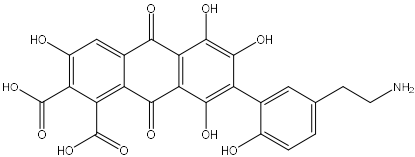
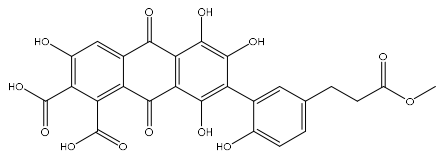


© 2020 by the authors. Submitted for possible open access publication under the terms and conditions of the Creative Commons Attribution (CC BY) license (<http://creativecommons.org/licenses/by/4.0/>).

## Supplementary file

Code	Compound / Ligand Name	Structure
DG01	Orange B	 <p>The structure of Orange B consists of a central benzimidazole ring system. One nitrogen atom is substituted with a 4-sulfamoylphenyl group (a benzene ring with a -SO<sub>2</sub>OH group at the para position). The other nitrogen atom is substituted with a 2-ethoxyacetyl group (-COOEt). The 2-position of the benzimidazole ring is substituted with a 5-sulfamoyl-1-naphthylamino group (a naphthalene ring with a -SO<sub>2</sub>OH group at the 5-position and an -NH- group at the 1-position).</p>
DG02	Cochineal Red A	 <p>The structure of Cochineal Red A is a complex polycyclic molecule. It features a central naphthalene ring system. One of the naphthalene rings is substituted with a sulfamoyl group (-SO<sub>2</sub>OH) at the 5-position. The other naphthalene ring is substituted with a sulfamoyl group (-SO<sub>2</sub>OH) at the 1-position and a sulfamoyl group (-SO<sub>2</sub>OH) at the 8-position. The central naphthalene ring is also substituted with a sulfamoyl group (-SO<sub>2</sub>OH) at the 4-position.</p>
DG03	Erythrosine	 <p>The structure of Erythrosine is a complex polycyclic molecule. It features a central naphthalene ring system. One of the naphthalene rings is substituted with a hydroxyl group (-OH) at the 5-position and an iodine atom (-I) at the 6-position. The other naphthalene ring is substituted with a hydroxyl group (-OH) at the 1-position and an iodine atom (-I) at the 2-position. The central naphthalene ring is also substituted with a hydroxyl group (-OH) at the 4-position.</p>
DG04	Laccaic Acid A	 <p>The structure of Laccaic Acid A is a complex polycyclic molecule. It features a central naphthalene ring system. One of the naphthalene rings is substituted with a hydroxyl group (-OH) at the 5-position and a hydroxyl group (-OH) at the 6-position. The other naphthalene ring is substituted with a hydroxyl group (-OH) at the 1-position and a hydroxyl group (-OH) at the 2-position. The central naphthalene ring is also substituted with a hydroxyl group (-OH) at the 4-position. The molecule also contains a carboxylic acid group (-COOH) and a hydroxyl group (-OH) on the right side.</p>
DG05	Laccaic Acid B	 <p>The structure of Laccaic Acid B is a complex polycyclic molecule. It features a central naphthalene ring system. One of the naphthalene rings is substituted with a hydroxyl group (-OH) at the 5-position and a hydroxyl group (-OH) at the 6-position. The other naphthalene ring is substituted with a hydroxyl group (-OH) at the 1-position and a hydroxyl group (-OH) at the 2-position. The central naphthalene ring is also substituted with a hydroxyl group (-OH) at the 4-position. The molecule also contains a carboxylic acid group (-COOH) and a hydroxyl group (-OH) on the right side.</p>

<p>DG06</p>	<p>Azorubine</p>	 <p>The structure shows two naphthalene rings connected by an azo (-N=N-) bridge. Each naphthalene ring has a sulfonic acid group (-SO<sub>3</sub>H) and a hydroxyl group (-OH) attached to it.</p>
<p>DG07</p>	<p>Quinoline yellow</p>	 <p>The structure consists of a quinoline ring system (a benzene ring fused to a pyridine ring) attached to a five-membered ring containing two carbonyl groups (=O).</p>
<p>DG08</p>	<p>Patent Blue V</p>	 <p>The structure features a central carbon atom double-bonded to a benzene ring with a diethyliminium group (=N<sup>+</sup>(Et)<sub>2</sub>) and single-bonded to another benzene ring with a diethylamino group (-N(Et)<sub>2</sub>). A third benzene ring is attached to the central carbon, bearing two sulfonic acid groups (-SO<sub>3</sub>H) and a hydroxyl group (-OH).</p>
<p>DG09</p>	<p>Laccaic Acid C</p>	 <p>The structure shows a complex polycyclic system with multiple hydroxyl groups (-OH) and a carboxylic acid group (-COOH). It includes a side chain with an amino group (-NH<sub>2</sub>) and a carboxylic acid group (-COOH).</p>
<p>DG10</p>	<p>Laccaic Acid D</p>	 <p>The structure is a polycyclic system with several hydroxyl groups (-OH) and a carboxylic acid group (-COOH) attached to the rings.</p>
<p>DG11</p>	<p>Tartrazine</p>	 <p>The structure features a central pyrazolone ring system with a carboxylic acid group (-COOH) and two sulfonic acid groups (-SO<sub>3</sub>H) attached to it.</p>

<p>DG12</p>	<p>Sunset yellow</p>	 <p>The chemical structure of Sunset yellow is a triphenylmethane dye. It consists of a central carbon atom double-bonded to a naphthalene ring and single-bonded to two phenyl rings. The naphthalene ring has a hydroxyl group (-OH) at the 1-position and a sulfonic acid group (-SO<sub>3</sub>H) at the 4-position. One of the phenyl rings has a sulfonic acid group (-SO<sub>3</sub>H) at the para position, and the other phenyl ring is unsubstituted.</p>
<p>DG13</p>	<p>Indigo Carmine</p>	 <p>The chemical structure of Indigo Carmine is a bis-indole dye. It features two indole-2,3-dione rings connected at their 2-positions. Each indole ring has a sulfonic acid group (-SO<sub>3</sub>H) at the 6-position.</p>
<p>DG14</p>	<p>Laccaic Acid E</p>	 <p>The chemical structure of Laccaic Acid E is a complex polycyclic molecule. It features a central naphthoquinone core with multiple hydroxyl groups (-OH) and carboxylic acid groups (-COOH). It is substituted with a 2-aminoethyl group (-CH<sub>2</sub>-CH<sub>2</sub>-NH<sub>2</sub>) on one of the phenyl rings.</p>
<p>DG15</p>	<p>Laccaic Acid F</p>	 <p>The chemical structure of Laccaic Acid F is similar to Laccaic Acid E, but instead of an amino group, it features a methyl ester group (-CH<sub>2</sub>-CH<sub>2</sub>-COOCH<sub>3</sub>) on one of the phenyl rings.</p>